Chemical Science

Accepted Manuscript

ROYAL SOCIETY OF CHEMISTRY

rsc.li/chemical-science

View Article Online
DOI: 10.1039/C6SC05619A

Achieving Efficient Violet-Blue Electroluminescence with CIE_y < 0.06 and EQE > 6% from Naphthyl-Linked Phenanthroimidazole-Carbazole Hybrid Fluorophores

Wen-Cheng Chen,[a] Yi Yuan,[ab] Shao-Fei Ni,[c] Qing-Xiao Tong,*[b] Fu-Lung Wong,[a] Chun-Sing Lee*[a]

[a] Center of Super-Diamond and Advanced Films (COSDAF) and Department of Biology and Chemistry, City University of Hong Kong, Hong Kong SAR, PR China
E-mail: apcslee@cityu.edu.hk
[b] Department of Chemistry and Key Laboratory for Preparation and Application of Ordered Structural Materials of Guangdong Province, Shantou University, 243 University Road, Shantou, Guangdong, 515063, PR China
E-mail: qxtong@stu.edu.cn
[c] Department of Chemistry, Southern University of Science and Technology, Shenzhen, 518055, PR China

Abstract:

In this work, we revealed a new approach for developing efficient violet-blue-emitting materials featured with hybrid local and charge transfer (HLCT) excited state through incorporation of naphthyl group(s) as a weak n-type π spacer in a donor-π-acceptor (D-π-A) system. The resulting materials (TPINCz and TPIBNCz) show improved intramolecular charge transfer properties and highly efficient violet-blue fluorescence. It is demonstrated that the pattern of the π spacers has significant influences on photophysical properties. The incorporation of a naphthyl/binaphthyl spacer between donor and acceptor moieties can alleviate a common dilemma that enhancing device performance by increasing charge transfer excited properties often leads to red-shifted emissions. A device using TPINCz as an emissive dopant shows a violet-blue emission with CIE coordinates of (0.153, 0.059) and a record high EQE of 6.56 ± 0.11% at a brightness of 1,000 cd m^{-2}. To the best of our knowledge, this performance is the highest among the reported devices with $CIE_y \leq 0.08$. Our study provides a new pathway for designing high-performance violet-blue emitters with a D-π-A architecture in organic electroluminescence application.

Introduction

The dramatic progress in the area of organic optoelectronics, observed over the last couple of decades, has been largely realized by the successful advance in numerous conjugated organic

View Article Online
DOI: 10.1039/C6SC05619A

materials, showing a wide range of tunable electrical/photo physical characteristics.[1–7] Understanding the structure-property relationship and mastering the ways to manipulate these unique properties significantly leads to a rapid development in organic semiconductor based applications, such as organic field-effect transistors, photovoltaic and electroluminescence (EL) devices *etc*. In the area of light generation, considerable interest in organic light-emitting devices (OLEDs) is derived from their attractive prospects as a new generation of full-color flat-plat display and solid-state lighting technologies.[8–10] Efficient violet-blue EL is very important in OLEDs since violet-blue fluorophores can be employed as energy donors to generate light covering the entire visible region and white light emission.[11–13] Additionally, efficient short-wavelength EL plays a key role in reducing power consumption and expanding the color gamut in full-color displays.[14,15] OLEDs with short-wavelength emission also has promising applications in other fields, such as chemical and biological sensing,[16] phototherapy,[17] photocopying,[18] high-density information storage,[19] sterilization[20] *etc.* Therefore, development of high-performance violet-blue light-emitting materials is crucial for the burgeoning OLED technology.

However, unlike their red, green and sky-blue counterparts with desirable performances, to date, reports on efficient organic fluorophores with deep-blue or violet-blue emission in the Commission Internationale de L'Eclairage (CIE) map matching or surpassing the high-definition television (HDTV) standard blue index (CIE coordinates of (0.15, 0.06)) are rare.[21,22] In principle, violet-blue emission requires materials with wide optical gap, which implies large HOMO (highest occupied molecular orbital)-LUMO (lowest unoccupied molecular orbital) offset, leading to inferior carrier injections. Moreover, the corresponding molecular conjugation must be strictly controlled. This often in turn results in drop of photoluminescence quantum yield (Φ_f) and poor electrical properties. These also cause difficulty in molecular design and synthesis for better thermal and morphological stability.[23,24]

In the past decade, much effort has been devoted to exploit a wide range of blue fluorescent dyes. For instance, Gao *et al.* developed a phenanthro[9,10-*d*]imidazole (PI) derivative and applied it in a violet-blue OLED exhibiting CIE coordinates of (0.166, 0.056), but the maximum external quantum efficiency (EQE) was only 3.02%.[25] Zhang *et al.* reported a blue emitter TBPMCN that can utilize ~100% excitons in a non-doped device.[26] This OLED

View Article Online
DOI: 10.1039/C6SC05619A

showed high performance with an EQE_{max} of 7.8% and a sky-blue EL emission (CIE coordinates of (0.16, 0.16)). An effective violet-blue OLED based on a silicon containing compound SiPIM was reported, which realized an EQE of 6.29% and a superior color index of (0.163, 0.040).[27] Unfortunately, the non-conducting silicon molecular framework of SiPIM leads to a high turn-on voltage (V_{on}, 4.2 V) and low power efficiency (PE). So far, the most effective violet-blue OLED was from a donor-acceptor (D-A) molecule with bisanthracene as an emitting core, showing an EQE up to 12% and a color purity of (0.15, 0.06).[28] It is suggested that triplet fusion (TF) is responsible for such a high EL performance. Another efficient deep-blue OLED reported by Adachi's group employed a sulfone/carbazole hybrid emitter that can emit thermally activated delayed fluorescence (TADF) with a maximum EQE of 9.9% and CIE coordinates of (0.15, 0.07).[29] Very recently, Hatakeyama and co-workers designed an ultrapure blue TADF-based emitter DABNA-1; its HOMO/LUMO can be separated interatomically, which endows the corresponding device with a high EQE of 13.5% and narrow blue EL spectra having CIE coordinates of (0.13, 0.09).[30] Nevertheless, such high efficiencies from the above-mentioned devices suffered from serious efficiency roll-off at high luminances (*e.g.* 1,000 cd m^{-2}), resulting in compromised performance at applicable brightness. To date, few reports for highly efficient deep-blue OLEDs matching or approaching the HDTV standard with slow efficiency roll-off are available, except a handful of recent literatures.[31–33]

Generally, common fluorescent dyes mainly rely on π-π* transition upon excitation, and emit highly efficient fluorescence from their locally excited (LE) states.[34] However, spin flip does not exist in OLEDs based on LE-based emitters due to strong hole-electron pairs with a high exciton binding energy (~ 1 eV),[35] causing relatively low electron-to-photon conversion efficiency. On the other hand, charge transfer (CT) exciton, another type of excited species with loosely bounded nature (~ 10 meV),[35] typically in D-A based molecular structures, can facilitate spin flip upon electrical charge injection and promote the exciton utilization efficiency (η_{exc}) significantly.[36] Nevertheless, CT emitters with strong D-A structures often show red-shifted emissions accompanied with broad full-widths at haft-maximum (FWHM), which is detrimental for deep-blue color purity.[23] Furthermore, low Φ_f is another drawback because of the lack of overlap between frontier molecular orbitals.[37] High Φ_f and η_{exc} are two

View Article Online
DOI: 10.1039/C6SC05619A

prerequisites to obtain a decent EQE, but both of LE and CT emitters fail to meet these requirements separately. To take full advantage of LE and CT excitons simultaneously, Ma and colleagues have established a series of highly emissive D-A type fluorescent materials that can employ more than 25% η_{exc} without using long-lived excitons.[26,36,38] It is reported that moderate D-A pairs can lead to hybrid local and charge transfer (HLCT) excited state, which is responsible for achieving high Φ_f and large η_{exc}. In this excited system, loosely bounded excitons from upper CT-like triplet state can be converted to singlets via a "hot exciton" channel, then produce photons from LE-like singlet state.[39] With these advantages, it is highly promising to design deep-blue D-A fluorescent materials employing the concept of HLCT excited states. However, up till now OLEDs using emitters featured with HLCT excited states having CIE_y coordinates below 0.06 and EQEs over 5% are still rarely reported.

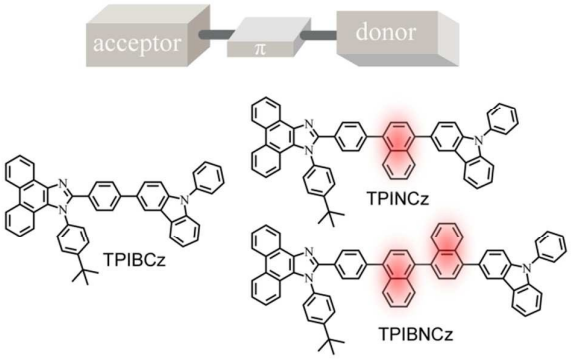

Scheme 1 Chemical structures of target D-π-A based fluorophores.

In this work, we report three D-π-A based PI-carbazole hybrid fluorophores—TPIBCz, TPINCz and TPIBNCz—with different π-linking moieties, and applied them as emitting core in violet-blue OLEDs (Scheme 1). To obtain HLCT-based short-wavelength emitting molecules, D and A have to be carefully selected to obtain appropriate electron push-pull strength such that both LE and CT excited states can be simultaneously achieved. In this molecular design, PI is chosen as a mild electron withdrawing group, while N-phenyl-9*H*-carbazole serves as a moderate electron donating segment. PI and carbazole are both rigid planar groups, which are beneficial to achieving high Φ_f. We also systematically studied the influence of π spacers, with different length and size between the D and the A

View Article Online
DOI: 10.1039/C6SC05619A

moieties, on their photophysical properties and EL performances. All the materials emit efficient violet-blue light and show excellent EL performances. It is worth noting that the OLED based on TPINCz as an emissive dopant exhibits a violet-blue color index of (0.153, 0.059) and a high efficiency with EQE up to 6.96 ± 0.08%. In a practical luminance of 1,000 cd m^{-2}, the EQE is still up to 6.56 ± 0.11%, which is the highest value among the blue OLEDs with CIE_y coordinates below 0.08.

Results and discussion

Synthesis and characterization

Synthesis of the three new fluorescence materials is shown in Scheme S1 in the Electronic Supplementary Information. First, the key intermediates AdhN-Br and AdhBN-Br were prepared by asymmetrical Suzuki reactions between bibromo naphthyl starting materials and (4-formylphenyl)boronic acid under mild conditions.[40] Then bromated PI derivatives TPI-Br, TPIN-Br and TPIBN-Br were synthesized via "one-pot" reactions.[41] The mixture of an aromatic aldehyde (4-bromobenzaldehye, AdhN-Br or AdhBN-Br), phenanthrene-9,10-dione, 4-(*tert*-butyl)aniline, and ammonium acetate were reacted in refluxing CH_3COOH under Ar for 10 h. At last, target compounds were obtained by Suzuki reactions from bromated PI intermediates (TPI-Br, TPIN-Br and TPIBN-Br) and (N-phenyl-9*H*-carbazol-3-yl)boronic acid with good yields. The new compounds were characterized and determined by $^1H/^{13}C$ NMR and mass spectroscopy.

Thermal properties

Thermal properties of the new materials were characterized by thermogravimetric analysis (TGA) and differential scanning calorimetry (DSC) in a nitrogen atmosphere. The relevant data are listed in Table 1. Joule heat, which results from carrier injection among interfacial heterojunctions and non-radiative energy loss, is common in operating devices.[42] Thus good thermal stability is of high significance for an OLED. Bulky and rigid structures of the new compounds are derived from the bulky conjugated backbone of PI and carbazole. The naphthyl-based compounds are more heat-resisting, with higher T_ds (5% weight loss

View Article Online
DOI: 10.1039/C6SC05619A

temperatures) of 480 and 510 °C (for TPINCz and TPIBNCz, respectively) over 439 °C of TPIBCz (Fig. 1). Moreover, TPINCz and TPIBNCz have high ash values upon heating to 800 °C, nevertheless TPIBCz experiences completely weight loss, demonstrating that adoption of naphthyl group is good for thermal stability.[43] High glass transition temperatures (T_g, inset of Fig. 1) also indicate superior thermal stability of the as-designed materials, which are competent for general device fabrication and operation.

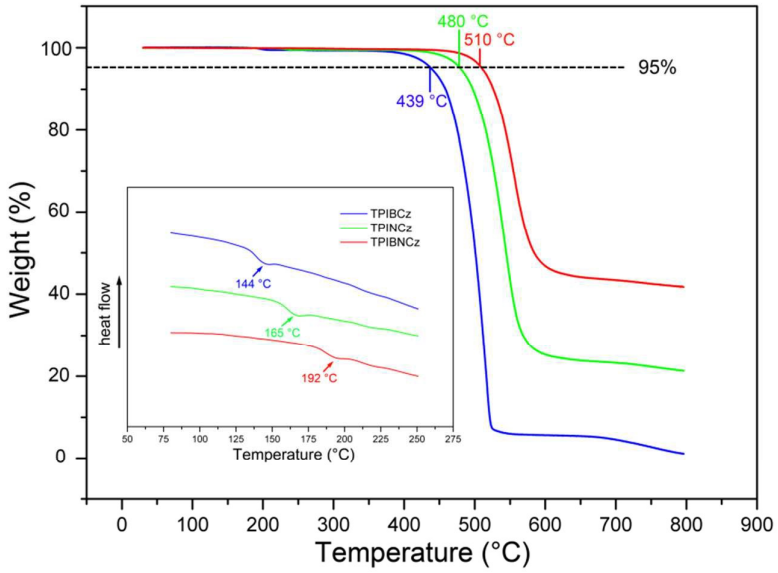

Fig. 1 Thermal properties of the new materials.

Table 1. Physical properties of TPIBCz, TPINCz and TPIBNCz.

Compd.	T_d[a] (°C)	T_g[b] (°C)	E_g[c] (eV)	HOMO[d] (eV)	LUMO[e] (eV)	λ_{abs}[f] (nm)	λ_{em}[f] (nm)	Φ_f[f] (%)
TPIBCz	439	144	3.04	-5.33	-2.29	338, 367 / 344, 370	395, 417, 428 / 414	85.2 / 64.2
TPINCz	480	165	3.06	-5.50	-2.44	335, 364 / 344, 369	428 / 450	~100 / 90.5
TPIBNCz	510	192	3.14	-5.54	-2.40	334, 364 / 336, 368	425 / 433	~100 / 96.8

[a] Decomposition temperature (5% weight loss). [b] Glass transition temperature. [c] Optical energy gap estimated from absorption onset in solid film. [d] Measured by cyclic voltammetry. [e] Calculated from LUMO = HOMO + E_g. [f] Measured in THF solution (10^{-6} mol L^{-1}) and solid film (30 nm), respectively.

Theoretical calculations

Theoretical calculations using density functional theory (DFT) method on B3LYP/6-31g(d,p)

View Article Online
DOI: 10.1039/C6SC05619A

level are performed to study the structure-property relationship of the new compounds. All the three compounds show similar molecular configurations apart from the central π-conjugated segments (Fig. S1). Because the naphthyl group can provide a large steric hindrance, TPINCz and TPIBNCz have more twisted configurations than TPIBCz.[43] This indicates that TPINCz and TPIBNCz can generate comparable emission to TPIBCz, although adoption of naphthyl group seems to extend the whole molecular conjugation to some degree.

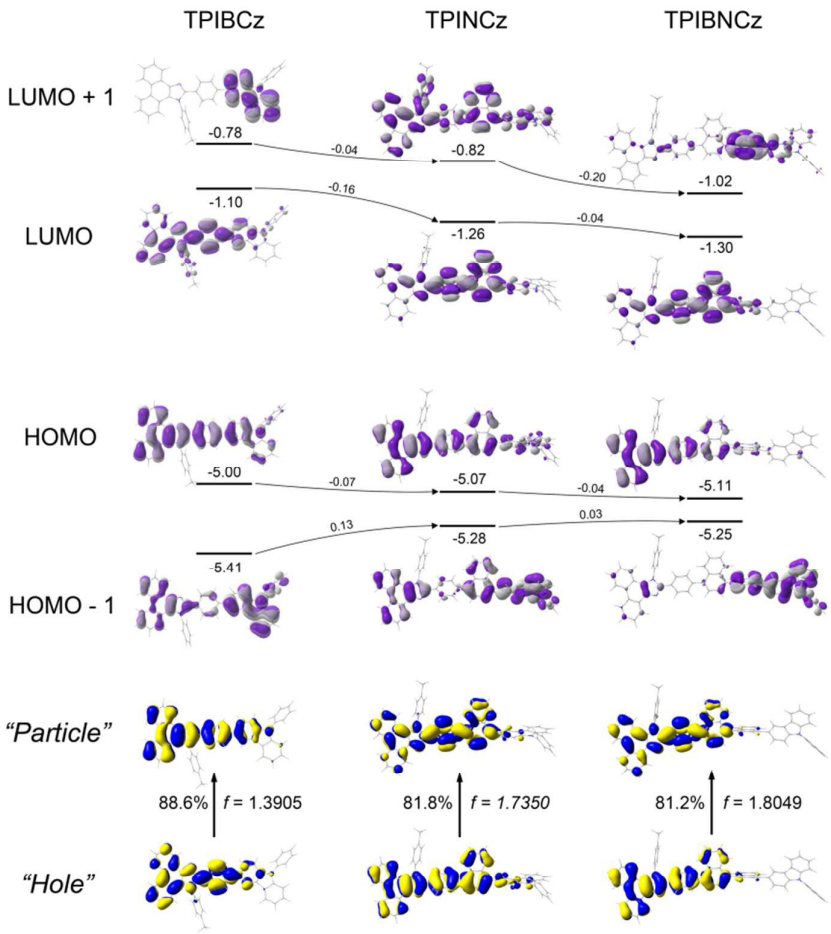

Fig. 2 Spatial distributions of the molecular orbitals and $S_0 \rightarrow S_1$ natural transition orbitals.

Fig. 2 shows spatial distributions of the molecular orbitals of the new compounds. Except for TPIBNCz, HOMOs of the other two molecules delocalize over the whole molecular frameworks with little contribution from the 4-(*tert*-butyl)phenyl group. The

View Article Online
DOI: 10.1039/C6SC05619A

HOMO energy levels of the three compounds have slight differences, while those of HOMO-1 gradually shift from -5.41 eV of TPIBCz to -5.25 eV of TPIBNCz. In addition, we note that the energy offsets between the HOMO and the HOMO-1 energy level become narrower from TPIBCz to TPIBNCz, leading to a pseudo-degenerate orbital pair in TPIBNCz. On the other hand, because of the incorporation of the naphthyl group with relatively large electron affinity,[44] energy levels of the LUMO and the LUMO+1 are deepened progressively, which is good for electron injection. Differences are also reflected in the orbital distribution, with naphthyl/binaphthyl group dominates the electron density of LUMOs in TPINCz and TPIBNCz. The naphthyl/binaphthyl group acts a week n-type π-linker in the D-π-A molecular design, and plays a key role in manipulating photophysical property, which will be discussed later. Unlike the completely separated HOMO/LUMO distributions in the strong D-A based molecules, the relatively weak electron pushing and pulling strengths of the D and the A lead to partially HOMOs/LUMOs overlaps in the present new compounds. TPINCz and TPIBNCz display more CT-like properties compared with TPIBCz due to the weak electron-withdrawing naphthyl group.

Natural transition orbital (NTO)[45] analysis was implemented by time-dependent DFT (TD-DFT) calculations (based on TD-M062X/6-31G(d,p)) to further investigate the excited state properties. As shown in Fig. 2, both "hole" and "particle" are distributed on the PI and the central π-linking moieties for S_0 (singlet ground state)→S_1 (first singlet excited state) transitions in the three molecules, with little contribution from the N-phenyl-9*H*-carbazole. It indicates that PI may be an active emitting core, and the central π-linking pattern can influence photophysical properties significantly. For TPIBCz, "hole" and "particle" seem to be located on the same part of the molecule, but π spacer contributes more in "hole" distribution. In comparison, "hole" and "particle" distributions have certain superposition in moiety from PI to naphthalene, but separated in the phenyl group between PI and naphthalene in TPINCz and TPIBNCz. The NTO analysis indicates that the three molecules may have LE characters and show partial CT features for S_0→S_1 transition. In addition, introduction of naphthalene also enhances the oscillator strength (*f*), which helps to maintain high Φ_fs.[46]

Photophysical properties

View Article Online
DOI: 10.1039/C6SC05619A

UV-vis absorption and photoluminescence (PL) spectra of the new compounds are shown in Fig. 3. The relative data are summarized in Table 1. In diluted THF solution, TPIBCz, TPINCz and TPIBNCz exhibit similar absorption bands, where the peaks between 330 and 340 nm are ascribed to the π-π* transition of the 2-substituent of imidazole to the PI group, while the sub-bands at longer wavelength region (~ 365 nm) are originated from PI's π-π* transition.[47] There are no evident broad absorptions, implying that the S_0s are of negligible CT feature. The absorptions in solid film on quartz show slight red-shifted spectra to those of solutions. From the absorption onsets, optical energy gaps (E_gs) are estimated to be 3.04, 3.06 and 3.14 eV, for TPIBCz, TPINCz and TPIBNCz, respectively. More twisted configurations induced by the naphthyl spacers may be responsible for the wider E_gs in TPINCz and TPIBNCz. Combined with the results from cyclic voltammetry (Fig. S2), in which HOMO levels are measured to be -5.33, -5.50 and -5.54 eV respectively, the LUMO levels are calculated to be -2.29, -2.44 and -2.40 eV for TPIBCz, TPINCz and TPIBNCz, respectively. All the materials can emit intense violet-to-blue fluorescence in diluted THF solution, but show quite different PL spectra. TPIBCz displays the highest energy emission in violet-blue region with fine structural peaks maximized at 417 nm, which is similar to those observed in isolated phenyl-substituted PI.[48,49] The relative Φ_f was measured to be 85.2%. Conversely, adding a naphthyl or binaphthyl to the π spacer results in structureless, red-shifted and relatively broad emissive bands stemmed from the effects of conjugated extension and improved CT processes in transitions. Fluorescences of TPINCz and TPIBNCz are very efficient, with Φ_fs approaching unity in THF solution. Interestingly, TPIBNCz with longer conjugated dimension has shorter-wavelength emission than TPINCz. It indicates that effect of conjugated confinement induced by the large dihedral angle in the two-fold-naphthyl spacer dominates the influence of conjugated extension after inserting another naphthyl. This nicely meets the demand of molecular design for violet-blue emitters. In vacuum-evaporated solid films prepared on clean quartz, although slight red shifts in emission are observed, the influence of close packing on emission is not significant, as evidenced by the high Φ_fs (see Table 1) and relatively narrow emission bands different from the typical excimer's PL spectra.[50] TPIBCz's film also exhibits LE-like vibrational fine emission bands with main peak at 414 nm. TPINCz shows the largest red shift in emission (peak at 450 nm), which results

View Article Online
DOI: 10.1039/C6SC05619A

from polarization effect in solid.[51] It implies that excited state of TPINCz is more sensitive to polarity of medium than TPIBCz.

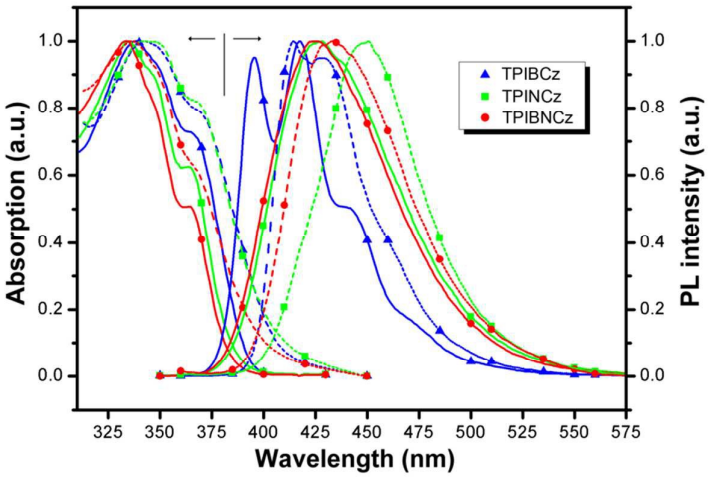

Fig. 3 Absorption and PL spectra of TPIBCz, TPINCz and TPIBNCz; solid line and dash line are for THF solution (~10^{-6} mol L^{-1}) and vacuum-evaporated film (30 nm), respectively.

To further study the excited state properties, solvation effects on photophysical properties were investigated in solvents with different polarities (Fig. 4a and Fig. S3-5). Upon increasing the solvent polarities gradually from *n*-hexane to acetonitrile (ACN), TPIBCz constantly displays a sharp emission band, and exhibits a slight red shift of 8 nm, which is responsible for polarity-insensitive LE transition. For TPINCz and TPIBNCz, on the contrary, their PL spectra not only exhibit significant red shifts, but also progressively broadened structureless bands as orientation polarization (Δf) of solvent increases. Compared with TPIBCz, such solvatochromic PL behavior in TPINCz and TPIBNCz implies CT properties in excited states.[52] The distinction of solvatochromic effect in TPIBCz and TPINCz/TPIBNCz is also in accord with the hypothesis by calculated results that the different properties of excited state are induced by the naphthyl spacers. Based on the Lippet-Mataga model,[53,54] we further estimated the dipole moments of excited state (μ_e) from the linear fitting analysis of the Stokes shift (ν_a-ν_f) and Δf. As shown in Fig. 4b, all the three materials display two-section linear relations in low and high Δf regions, but the slopes of individual fittings are different. The two slopes for TPIBCz's fittings are estimated to be 8.2 D and 13.9 D, for low and high Δf regions, respectively. Based on the small μ_es, TPIBCz shows a LE excited state in the

View Article Online
DOI: 10.1039/C6SC05619A

region of small Δf and a LE-dominating HLCT excited state in the region of large Δf. In contrast, although relatively small μ_es are obtained in TPINCz and TPIBNCz (12.6 and 9.6 D, respectively) in solvents with small Δf values, steep slopes are evident in solvents of high Δf values, corresponding to μ_es of 18.0 and 20.1 D, respectively. The large μ_es can be treated as CT-like characters. TPINCz and TPIBNCz show a mixture of LE and CT excited properties, namely HLCT excited states. On the other hand, the two fitted lines for TPINCz show smaller difference in their slopes comparing to those for TPIBNCz. With this observation, we speculate that LE and CT excited states mix better in the former. In the previous publications, efficient HLCT excited states in blue emitters are generally achieved by the means of connecting different donor and acceptor moieties with single bond,[55] different π-linking modes or tuning the strength of electron donating/withdrawing in D/A pairs.[26] In contrast, we can easily obtain accessible deep-blue emitters featured with HLCT excited states by incorporation of a naphthyl/binaphthyl spacer with weak n-type nature and high twisting angles in π linking moiety, and this strategy can be applied to modify the common D-π-A to invoke HLCT excited state.

View Article Online
DOI: 10.1039/C6SC05619A

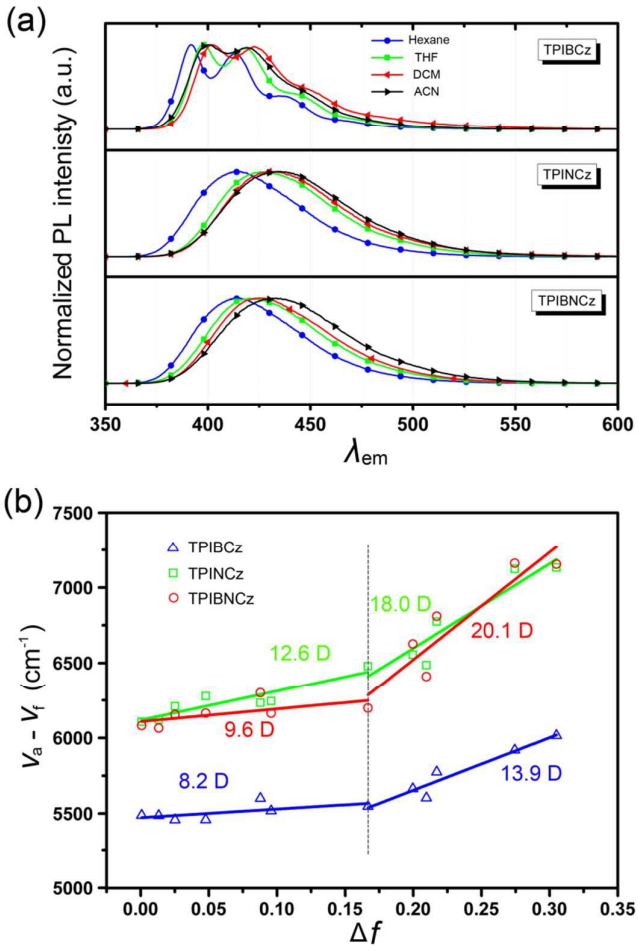

Fig. 4 (a) Solvatochromic PL spectra of TPIBCz, TPINCz and TPIBNCz in solvents with increasing polarities; (b) Linear fitting based on Lippert-Mataga model in various solvents.

Electrical properties

Electrical properties of the three fluorophores were studied in single carrier-only type devices. The structure of hole-only devices is indium tin oxide (ITO)/ N,N'-bis-(1-naphthalenyl)-N,N'-bis-phenyl-(1,1'-biphenyl)-4,4'-diamine (NPB, 10 nm)/ one of the new compounds (70 nm)/ NPB (10 nm)/ Al (150 nm), and the electron-only devices have a structure of ITO/ 2,9-dimethyl-4,7-diphenyl-1,10-phenanthroline (BCP, 10 nm)/ one of the new compounds (70 nm)/ BCP (10 nm)/ LiF (1 nm)/ Al (150 nm). The current density-voltage (*J-V*) curves are shown in Fig. S6. Obviously, similar to most of the common organic semiconductors, the compounds have much better conductivity for hole than for electron. The

View Article Online
DOI: 10.1039/C6SC05619A

relatively low hole transporting property of TPIBNCz may be caused by the highly twisting molecular configuration, as such geometry is not beneficial to charge flowing intramolecularly. On the other hand, the planar molecule TPIBCz has the highest electron mobility. The TPINCz-based electron-only device has lower current density than its TPIBNCz counterpart. This can be attributed to the incorporation of the binaphthyl spacer can enhance LUMO overlap in solid, although the highly twisting geometry more or less hinders charge transport.[43]

Electroluminescence performances

To evaluate the EL performances of the new materials as emitting cores, we initially fabricated three non-doped OLEDs with a structure of ITO/ NPB (70 nm for the TPIBCz and the TPIBNCz based devices, 50 nm for the TPINCz based OLED)/ TcTa (tris(4-carbazoyl-9-ylphenyl)amine, 5 nm)/ one of the emitters (30 nm)/ 1,3,5-tris(1-phenyl-1*H*-benzimidazol-2-yl)benzene (TPBi, 30 nm)/ LiF (1 nm)/ Al (100 nm), in which ITO is the transparent anode, NPB is used as a hole transporting layer, TcTa as a buffer and exciton confining layer,[24] TPBi as an electron transporting and hole blocking layer, LiF as an electron injection layer and Al is the cathode. Although the emitters used here have better hole than electron transporting properties, the unfavorable effects due to the unbalanced electron and hole currents are partly remedied by the exciton confining structures. The thin TcTa layer can hinder the hole flow in the device due to additional interfacial heterojunction, and confine the exciton in emissive layer original from its high E_g (~ 3.4 eV). Besides, the deep HOMO level (-6.30 eV) of TPBi can also block the hole in the devices. Fig. 5 shows the device performances, and key performance data are summarized in Table 2. The OLED using TPINCz displays the highest EQE of 5.95 ± 0.10% and deep-blue EL emission with CIE coordinates of (0.157, 0.084) (at 1,000 cd m^{-2}). It is worth noting that this device does not show serious efficiency roll-off. At a practical luminance of 1,000 cd m^{-2}, a high-level EQE of 5.83 ± 0.06% is still maintained. The maximum current efficiency (CE) and PE are up to 5.00 ± 0.14 cd A^{-1} and 5.15 ± 0.15 lm W^{-1}, respectively. The devices based on TPIBCz and TPIBNCz show slightly lower performances, having maximum EQEs of 3.38 ± 0.10% and 5.09 ± 0.13%, respectively. But their EL spectra shift to the shorter-wavelength region with

View Article Online
DOI: 10.1039/C6SC05619A

peaks at 435 and 436 nm, and the corresponding CIE coordinates are (0.154, 0.063) and (0.157, 0.074) at 1,000 cd m^{-2}, respectively. Fig S7 shows the EL and PL spectra of the non-doped devices and solid thin films respectively. Two types of spectra have slight difference in bandwidth which might be due to weak micro-cavity effects in the devices. The EL spectra are comparable to the solid film PL spectra, indicating that the devices emit intrinsic emission from the title fluorophores. It is suggested that the highest performances attained in TPINCz-based could be ascribed to the high CT component in the excited state and better hybridization of LE and CT states. Fig. S8 shows the calculated first-ten singlet and triplet energy levels of the three molecules. Some upper triplet states are close to their corresponding S_1s, like T_5/T_6, T_7 and T_9 for TPIBCz, TPINCz and TPIBNCz respectively. In addition, the NTOs of these high-lying triplet states exhibit complicated transitions with similar contributions and HLCT excited properties (Fig. S9-11). This implies that this high performance may be due to the potential "hot exciton" channels through reverse inter-system crossing (RISC) from upper triplet states to S_1 (red arrows in Fig. S8). Contribution to these high efficiencies from TF and TADF are considered to be insignificant. Linear relation of the luminance-current density (*L-J*) curves (Fig. S12) implies that few emissive triplet excitons via TF,[56] and large S_1 and T_1 energy gaps (Fig. S8) as well as certain HOMOs/LUMOs overlap (Fig. 2) indicate that the new molecules may not emit TADF.[7]

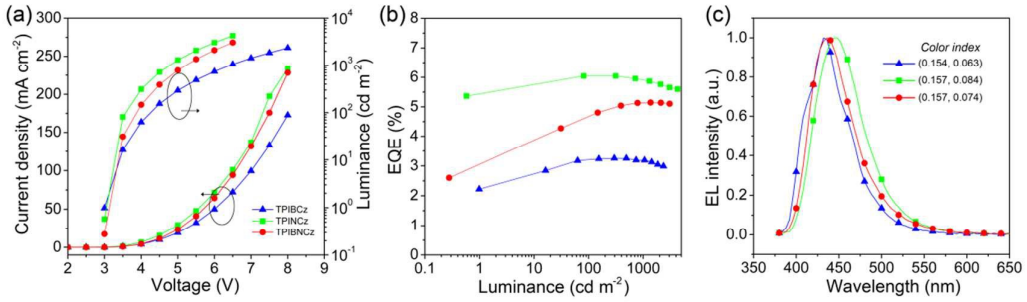

Fig. 5 (a) Current density-voltage-luminance characteristics, (b) EQE-luminance curves, (c) EL spectra of the TPIBCz, the TPINCz and the TPIBNCz based non-doped OLEDs.

Table 2 EL performances of the OLEDs based on TPIBCz, TPINCz and TPIBNCz.

Emissive layer	V_{on}[a] (V)	λ_{EL} (nm)	CIE[b] (x, y)	CE_{max}[c] (cd A^{-1})	PE_{max}[d] (lm W^{-1})	EQE_{max}[e] (%)
TPIBCz	3.0	435	0.154, 0.063	1.70 ± 0.02	1.44 ± 0.05	3.38 ± 0.10

View Article Online
DOI: 10.1039/C6SC05619A

TPINCz	3.1	448	0.157, 0.084	5.00 ± 0.14	5.15 ± 0.15	5.95 ± 0.10
TPIBNCz	3.2	436	0.157, 0.074	3.29 ± 0.08	2.80 ± 0.09	5.09 ± 0.13
10 wt% TPIBCz	3.7	428	0.156, 0.043	1.91 ± 0.02	1.72 ± 0.02	5.06 ± 0.05
20 wt% TPIBCz	3.3	432	0.156, 0.046	1.96 ± 0.02	1.68 ± 0.04	5.46 ± 0.07
30 wt% TPIBCz	3.2	432	0.156, 0.047	2.10 ± 0.04	2.20 ± 0.08	5.47 ± 0.10
10 wt% TPINCz	3.3	436	0.155, 0.054	3.02 ± 0.15	2.53 ± 0.20	6.60 ± 0.20
20 wt% TPINCz	3.1	440	0.153, 0.059	3.71 ± 0.11	3.71 ± 0.15	6.96 ± 0.08
30 wt% TPINCz	3.1	440	0.153, 0.062	3.75 ± 0.06	3.36 ± 0.05	6.71 ± 0.12
10 wt% TPIBNCz	3.4	424	0.158, 0.044	1.89 ± 0.05	1.51 ± 0.10	5.48 ± 0.15
20 wt% TPIBNCz	3.2	428	0.157, 0.048	2.34 ± 0.04	2.14 ± 0.04	5.99 ± 0.05
30 wt% TPIBNCz	3.1	428	0.157, 0.051	2.55 ± 0.05	2.24 ± 0.10	6.03 ± 0.14

[a] Voltage at 1 cd m^{-2}. [b] Detected at 1,000 cd m^{-2}. [c] Current efficiency, [d] power efficiency and [e] external quantum efficiency at maximum.

To further improve the efficiency and color purity, we also fabricated doped devices with a structure of ITO/ NPB (70 nm)/ TcTa (5 nm)/ CBP (4,4'-bis(N-carbazolyl)-1,1'-biphenyl): one of emitters (30 nm)/ TPBi (30 nm)/ LiF (1 nm)/ Al (100 nm). Influence of different doping levels (10, 20 and 30 wt%) on the device performances was investigated. CPB, a high-energy-gap compound, was chosen as a host material. In the host-guest system, efficiency can improved significantly due to efficient Förster energy transfer.[57] Besides, in the host matrix, better color purity, wider recombination zone and less non-radiative relaxation can be expected. Fig. 6a-c show the EL spectra of the devices. All the doped devices show obviously blue-shifted EL spectra compared with the corresponding non-doped devices. This can be mainly attributed to the decrease of the medium polarity, since CBP is a non-polar host material.[58] As the doping concentration decreases, finer structural EL spectra are observed in the TPIBCz-based devices, which is in accord with the LE-like photophysical behavior of TPIBCz. The corresponding CIE_y coordinate shifts from 0.063 (non-doped) to 0.043 (10 wt% in CBP). On the other hand, the EL spectra of the TPINCz and the TPIBNCz-based OLEDs are relatively more sensitive to doping ratios, which may be responsible for CT excited properties. For example, the EL spectra of the TPINCz-based doped devices show an evidently hypsochromic shift from deep-blue region (λ_{EL} = 448 nm, CIE: (0.152, 0.084)) in the non-doped device to violet-blue region (λ_{EL} = 436 nm, CIE: (0.155, 0.054)). Similar changes are observed in the TPIBNCz-based OLEDs. The doped devices show superior

View Article Online
DOI: 10.1039/C6SC05619A

violet-blue EL emission, their corresponding CIE_y coordinates range from ~ 0.04 to 0.06, even surpassing the standard blue for National Television System Committee (NTSC) of (0.14, 0.08) and HDTV of (0.15, 0.06), as shown in Fig. S13. Fig. 6d-f show the EQE-*L*-PE curves for the doped devices, and their *J*-*V*-*L* characteristics are shown in Fig. S14. The doped OLEDs show improved efficiency. The maximum EQE of the TPIBCz-based 10 wt% doped OLEDs reaches 5.06 ± 0.05%, comparing to the value of 3.38 ± 0.10% in the non-doped device. However, the V_{on} is raised to 3.7 V, mainly due to the larger energy gap of CBP. Upon increasing the doping concentration from 10 to 30 wt%, the device efficiency first increases and then nearly saturates at 30 wt%. The electrical property also followed this trend: current density is the highest and the V_{on} decreases to 3.2 V in the 30 wt% TPIBCz-based device. Similar changes are observed in the TPINCz and the TPIBNCz-based OLEDs. However, the EL spectra gradually shift to longer-wavelength region as the dopant concentration increases. Comprehensively speaking, we suggest that the optimized doping level is 20 wt%. Among all the device fabricated, the TPINCz-based doped device (20 wt%) exhibited the highest performance, with an EQE up to 6.96 ± 0.08% and a decent maximum PE of 3.71 ± 0.15 lm W^{-1}. The highest performance of the TPINCz-based device may be mainly ascribed to the better mixed LE and CT components, resulting in a more efficient HLCT excited. EL performances of the reported high-efficiency deep-blue OLEDs are summarized in Table S2, and illustrated in Fig. 7. [23,24,27,28,31–33,59–69] It can be seen that few OLEDs can emit efficient violet-blue light with EQE over 5% at a luminance of 1,000 cd m^{-2}. The OLEDs based on our new emitters exhibit superior efficiencies over most of the reported devices with $CIE_y < 0.08$ (NTSC standard) at a luminance of 1,000 cd m^{-2}. More importantly, the TPINCz-based doped OLED (red solid star) shows a champion performance with an EQE of 6.56 ± 0.11% at 1,000 cd m^{-2}.

View Article Online
DOI: 10.1039/C6SC05619A

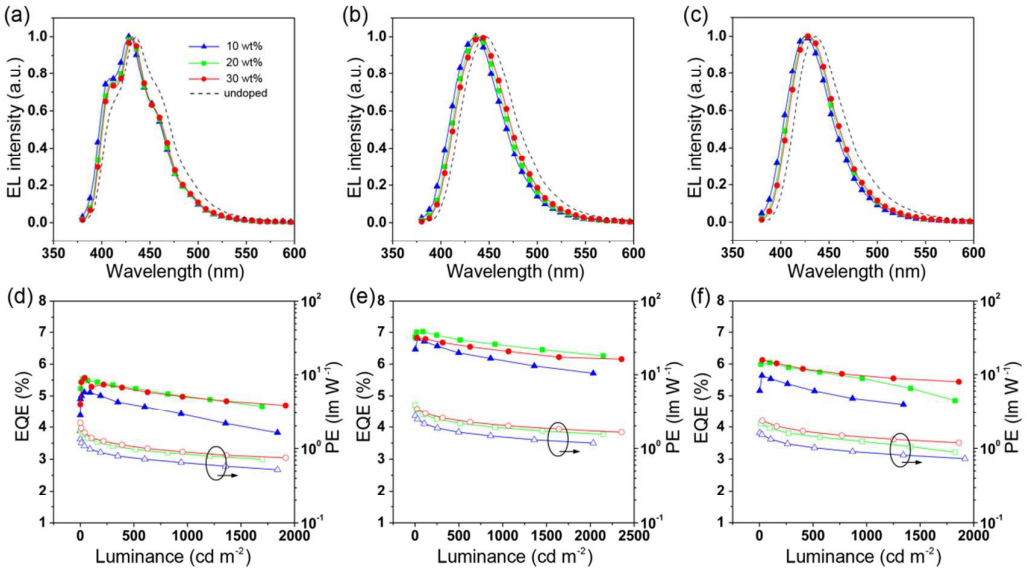

Fig. 6 EL spectra of the CBP-doped devices based on a) TPIBCz, b) TPINCz and c) TPIBNCz, respectively. EQE-luminance curves for the CBP-doped devices based on e) TPIBCz, f) TPINCz and g) TPIBNCz, respectively.

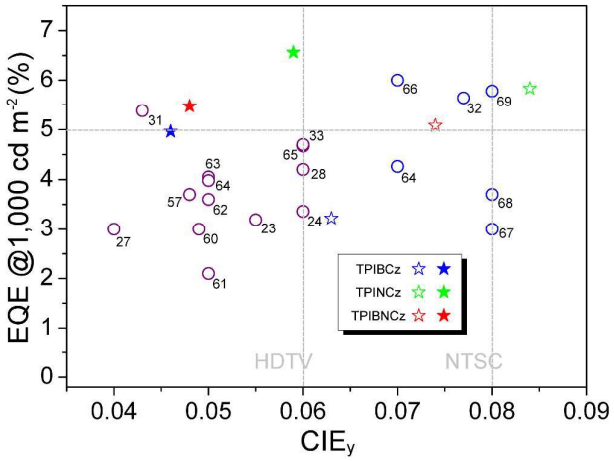

Fig. 7 A plot of EQE at 1,000 cd m^{-2} against CIE_y for the state-of-the-art deep-blue OLEDs with $CIE_y \leqslant 0.08$. Data points marked with empty circles and reference number are taken from published devices. Details of these devices are listed in the Electronic Supplementary Information (Table S2). Data point marked with empty and solid stars are devices in this work by using the three emitters in non-doped and doped emitting layers respectively.

View Article Online
DOI: 10.1039/C6SC05619A

Conclusions

We have designed and synthesized three D-π-A type PI-carbazole hybrid fluorophores: TPIBCz, TPINCz and TPIBNCz. It is found that the pattern of the π spacers have significant influences on photophysical properties and device performances. The incorporation of a naphthyl/binaphthyl group between 1-(4-(*tert*-butyl)phenyl)-2-phenyl-1*H*-phenanthro[9,10-*d*]imidazole and N-phenyl-9*H*-carbazole can alleviate a common dilemma that enhancing device efficiency by increasing CT excited properties often leads to red-shifted emission. Quantum calculations and photophysical experiments demonstrated that naphthyl-linked TPINCz and TPIBNCz show remarkable HLCT excited states, while TPIBCz exhibits a LE-dominating character. Our materials can emit violet-blue emission with high Φ_fs in solid, indicating that they are promising candidates for high-performance violet-blue emitters in OLED applications. The doped device of TPINCz shows violet-blue EL with CIE coordinates of (0.153, 0.059), which are very close to the HDTV blue color standard of (0.15, 0.06). Its maximum EQE can reach 6.96 ± 0.08%. Additionally, this value retains 94% of the peak value at a practical brightness of 1,000 cd m^{-2}, showing a very low efficiency roll-off. The performances of the OLEDs reported here are among the best value in the devices with $CIE_y \leq 0.08$. Our study may provide a new pathway for designing high-performance violet-blue emitters in OLED application.

Acknowledgement

CSL would like to acknowledge the supports from the Ministry of Science and Technology of China (Project No. 2016YFB0401002) and Guangdong Innovative and Entrepreneurial Research Team Program (Project Nos. 2013C090 and KYPT20141013150545116); QXT acknowledges the supports from the Natural Science Foundation of China (Project Nos. 51273108 and 51673113) and the National Basic Research Program of China (973 Program Nos. 2013CB834803).

View Article Online
DOI: 10.1039/C6SC05619A

References

1 C. W. Tang and S. A. VanSlyke, *Appl. Phys. Lett.*, 1987, **51**, 913–915.
2 S.-C. Lo and P. L. Burn, *Chem. Rev.*, 2007, **107**, 1097–1116.
3 M. Zhu and C. Yang, *Chem. Soc. Rev.*, 2013, **42**, 4963–4976.
4 C.-T. Chen, *Chem. Mater.*, 2004, **16**, 4389–4400.
5 R. C. Evans, P. Douglas and C. J. Winscom, *Coord. Chem. Rev.*, 2006, **250**, 2093–2126.
6 K. T. Kamtekar, A. P. Monkman and M. R. Bryce, *Adv. Mater.*, 2010, **22**, 572–582.
7 Y. Tao, K. Yuan, T. Chen, P. Xu, H. Li, R. Chen, C. Zheng, L. Zhang and W. Huang, *Adv. Mater.*, 2014, **26**, 7931–7958.
8 F. So, *Organic Electronics: Materials, Processing, Devices and Applications*, CRC Press, 2009.
9 H. Sasabe and J. Kido, *J. Mater. Chem. C*, 2013, **1**, 1699–1707.
10 B. W. D'Andrade and S. R. Forrest, *Adv. Mater.*, 2004, **16**, 1585–1595.
11 Q. Wang and D. Ma, *Chem. Soc. Rev.*, 2010, **39**, 2387–2398.
12 Z. Chen, X.-K. Liu, C.-J. Zheng, J. Ye, C.-L. Liu, F. Li, X.-M. Ou, C.-S. Lee and X.-H. Zhang, *Chem. Mater.*, 2015, **27**, 5206–5211.
13 J. Ye, Z. Chen, F. An, M. Sun, H.-W. Mo, X. Zhang and C.-S. Lee, *ACS Appl. Mater. Interfaces*, 2014, **6**, 8964–8970.
14 C. H. Chen, M.-T. Lee and C.-H. Liao, *SPIE Newsroom*, 2006, DOI: 10.1117/2.1200601.0012.
15 S.-W. Wen, M.-T. Lee and C. H. Chen, *J. Disp. Technol.*, 2005, **1**, 90.
16 J. Shinar and R. Shinar, *J. Phys. Appl. Phys.*, 2008, **41**, 133001.
17Z. Hao, J. Zhang, X. Zhang, X. Ren, Y. Luo, S. Lu and X. Wang, *J. Phys. Appl. Phys.*, 2008, **41**, 182001.
18 D. S. Thakare, S. K. Omanwar, P. L. Muthal, S. M. Dhopte, V. K. Kondawar and S. V. Moharil, *Phys. Status Solidi A*, 2004, **201**, 574–581.
19 H. van Santen and J. H. M. Neijzen, *Jpn. J. Appl. Phys.*, 2003, **42**, 1110–1112.
20 L. T. T. Nhung, H. Nagata, A. Takahashi, M. Aihara, T. Okamoto, T. Shimohata, K. Mawatari, M. Akutagawa, Y. Kinouchi and M. Haraguchi, *J. Med. Invest.*, 2012, **59**, 53–58.
21 X. Yang, X. Xu and G. Zhou, *J. Mater. Chem. C*, 2015, **3**, 913–944.
22 W.-C. Chen, C.-S. Lee and Q.-X. Tong, *J. Mater. Chem. C*, 2015, **3**, 10957–10963.
23 J. Ye, Z. Chen, M.-K. Fung, C. Zheng, X. Ou, X. Zhang, Y. Yuan and C.-S. Lee, *Chem. Mater.*, 2013, **25**, 2630–2637.
24 W.-C. Chen, G.-F. Wu, Y. Yuan, H.-X. Wei, F.-L. Wong, Q.-X. Tong and C.-S. Lee, *RSC Adv.*, 2015, **5**, 18067–18074.
25 Z. Gao, Y. Liu, Z. Wang, F. Shen, H. Liu, G. Sun, L. Yao, Y. Lv, P. Lu and Y. Ma, *Chem. – Eur. J.*, 2013, **19**, 2602–2605.
26 S. Zhang, L. Yao, Q. Peng, W. Li, Y. Pan, R. Xiao, Y. Gao, C. Gu, Z. Wang, P. Lu, F. Li, S. Su, B. Yang and Y. Ma, *Adv. Funct. Mater.*, 2015, **25**, 1755–1762.
27Z. Gao, G. Cheng, F. Shen, S. Zhang, Y. Zhang, P. Lu and Y. Ma, *Laser Photonics Rev.*, 2014, **8**, L6–L10.
28 J.-Y. Hu, Y.-J. Pu, F. Satoh, S. Kawata, H. Katagiri, H. Sasabe and J. Kido, *Adv. Funct. Mater.*, 2014, **24**, 2064–2071.
29 Q. Zhang, J. Li, K. Shizu, S. Huang, S. Hirata, H. Miyazaki and C. Adachi, *J. Am. Chem. Soc.*, 2012, **134**, 14706–14709.

View Article Online
DOI: 10.1039/C6SC05619A

30 T. Hatakeyama, K. Shiren, K. Nakajima, S. Nomura, S. Nakatsuka, K. Kinoshita, J. Ni, Y. Ono and T. Ikuta, *Adv. Mater.*, 2016, **28**, 2777–2781.

31 A. Obolda, Q. Peng, C. He, T. Zhang, J. Ren, H. Ma, Z. Shuai and F. Li, *Adv. Mater.*, 2016, **28**, 4740–4746.

32X. Tang, Q. Bai, Q. Peng, Y. Gao, J. Li, Y. Liu, L. Yao, P. Lu, B. Yang and Y. Ma, *Chem. Mater.*, 2015, **27**, 7050–7057.

33 I. Kondrasenko, Z.-H. Tsai, K. Chung, Y.-T. Chen, Y. Y. Ershova, A. Doménech-Carbó, W.-Y. Hung, P.-T. Chou, A. J. Karttunen and I. O. Koshevoy, *ACS Appl. Mater. Interfaces*, 2016, **8**, 10968–10976.

34 V. Ramamurthy and K. S. Schanze, *Organic photochemistry and photophysics*, CRC Press, 2005.

35 M. Pope and C. E. Swenberg, *Electronic Processes in Organic Crystals and Polymers*, Oxford University Press, 1999.

36 W. Li, Y. Pan, R. Xiao, Q. Peng, S. Zhang, D. Ma, F. Li, F. Shen, Y. Wang, B. Yang and Y. Ma, *Adv. Funct. Mater.*, 2014, **24**, 1609–1614.

37 A.-D. Gorse and M. Pesquer, *J. Phys. Chem.*, 1995, **99**, 4039–4049.

38 S. Zhang, W. Li, L. Yao, Y. Pan, F. Shen, R. Xiao, B. Yang and Y. Ma, *Chem. Commun.*, 2013, **49**, 11302–11304.

39 Y. Pan, W. Li, S. Zhang, L. Yao, C. Gu, H. Xu, B. Yang and Y. Ma, *Adv. Opt. Mater.*, 2014, **2**, 510–515.

40 N. Miyaura and A. Suzuki, *Chem. Rev.*, 1995, **95**, 2457–2483.

41 W.-C. Chen, Q.-X. Tong and C.-S. Lee, *Sci. Adv. Mater.*, 2015, **7**, 2193–2205.

42J.-R. Gong, L.-J. Wan, S.-B. Lei, C.-L. Bai, X.-H. Zhang and S.-T. Lee, *J. Phys. Chem. B*, 2005, **109**, 1675–1682.

43 W.-C. Chen, Y. Yuan, G.-F. Wu, H.-X. Wei, J. Ye, M. Chen, F. Lu, Q.-X. Tong, F.-L. Wong and C.-S. Lee, *Org. Electron.*, 2015, **17**, 159–166.

44 B. C. Lin, C. P. Cheng and Z. P. M. Lao, *J. Phys. Chem. A*, 2003, **107**, 5241–5251.

45 R. L. Martin, *J. Chem. Phys.*, 2003, **118**, 4775–4777.

46 Y. Sagara, K. Shizu, H. Tanaka, H. Miyazaki, K. Goushi, H. Kaji and C. Adachi, *Chem. Lett.*, 2014, **44**, 360–362.

47 Y. Zhang, S.-L. Lai, Q.-X. Tong, M.-F. Lo, T.-W. Ng, M.-Y. Chan, Z.-C. Wen, J. He, K.-S. Jeff, X.-L. Tang, W.-M. Liu, C.-C. Ko, P.-F. Wang and C.-S. Lee, *Chem. Mater.*, 2012, **24**, 61–70.

48M. Chen, Y. Yuan, J. Zheng, W.-C. Chen, L.-J. Shi, Z.-L. Zhu, F. Lu, Q.-X. Tong, Q.-D. Yang, J. Ye, M.-Y. Chan and C.-S. Lee, *Adv. Opt. Mater.*, 2015, **3**, 1215–1219.

49 W. Li, D. Liu, F. Shen, D. Ma, Z. Wang, T. Feng, Y. Xu, B. Yang and Y. Ma, *Adv. Funct. Mater.*, 2012, **22**, 2797–2803.

50 K.-C. Wu, P.-J. Ku, C.-S. Lin, H.-T. Shih, F.-I. Wu, M.-J. Huang, J.-J. Lin, I.-C. Chen and C.-H. Cheng, *Adv. Funct. Mater.*, 2008, **18**, 67–75.

51 V. Bulović, R. Deshpande, M. E. Thompson and S. R. Forrest, *Chem. Phys. Lett.*, 1999, **308**, 317–322.

52 Z. R. Grabowski, K. Rotkiewicz and W. Rettig, *Chem. Rev.*, 2003, **103**, 3899–4032.

53 E. Lippert, *Z. Für Elektrochem. Berichte Bunsenges. Für Phys. Chem.*, 1957, **61**, 962–975.

54 N. Mataga, Y. Kaifu and M. Koizumi, *Bull. Chem. Soc. Jpn.*, 1956, **29**, 465–470.

55 W. Li, Y. Pan, L. Yao, H. Liu, S. Zhang, C. Wang, F. Shen, P. Lu, B. Yang and Y. Ma, *Adv. Opt.*

View Article Online
DOI: 10.1039/C6SC05619A

Mater., 2014, **2**, 892–901.

56 A. P. Monkman, *ISRN Mater. Sci.*, 2013, **2013**, 670130.

57 J.-H. Jou, S. Kumar, A. Agrawal, T.-H. Li and S. Sahoo, *J. Mater. Chem. C*, 2015, **3**, 2974–3002.

58 J.-H. Jou, Y.-L. Chen, J.-R. Tseng, R.-Z. Wu, J.-J. Shyue, K. R. J. Thomas, N. Kapoor, C.-T. Chen, Y.-P. Lin, P.-H. Wang, H.-W. Hung, J.-Y. Li and S.-P. Chen, *J. Mater. Chem.*, 2012, **22**, 15500–15506.

59 J.-H. Jou, S. Kumar, P.-H. Fang, A. Venkateswararao, K. R. J. Thomas, J.-J. Shyue, Y.-C. Wang, T.-H. Li and H.-H. Yu, *J. Mater. Chem. C*, 2015, **3**, 2182–2194.

60 H. Liu, Q. Bai, L. Yao, H. Zhang, H. Xu, S. Zhang, W. Li, Y. Gao, J. Li, P. Lu, H. Wang, B. Yang and Y. Ma, *Chem. Sci.*, 2015, **6**, 3797–3804.

61 D. He, Y. Yuan, B. Liu, D.-Y. Huang, C.-Y. Luo, F. Lu, Q.-X. Tong and C.-S. Lee, *Dyes Pigments*, 2017, **136**, 347–353.

62 C. He, H. Guo, Q. Peng, S. Dong and F. Li, *J. Mater. Chem. C*, 2015, **3**, 9942–9947.

63 W.-C. Chen, Y. Yuan, G.-F. Wu, H.-X. Wei, L. Tang, Q.-X. Tong, F.-L. Wong and C.-S. Lee, *Adv. Opt. Mater.*, 2014, **2**, 626–631.

64 Y. Yuan, J.-X. Chen, F. Lu, Q.-X. Tong, Q.-D. Yang, H.-W. Mo, T.-W. Ng, F.-L. Wong, Z.-Q. Guo, J. Ye, Z. Chen, X.-H. Zhang and C.-S. Lee, *Chem. Mater.*, 2013, **25**, 4957–4965.

65 T. Shan, Y. Liu, X. Tang, Q. Bai, Y. Gao, Z. Gao, J. Li, J. Deng, B. Yang, P. Lu and Y. Ma, *ACS Appl. Mater. Interfaces*, 2016, **8**, 28771–28779.

66 C. Li, S. Wang, W. Chen, J. Wei, G. Yang, K. Ye, Y. Liu and Y. Wang, *Chem. Commun.*, 2015, **51**, 10632–10635.

67 X. Xing, L. Xiao, L. Zheng, S. Hu, Z. Chen, B. Qu and Q. Gong, *J. Mater. Chem.*, 2012, **22**, 15136–15140.

68 Y.-H. Chung, L. Sheng, X. Xing, L. Zheng, M. Bian, Z. Chen, L. Xiao and Q. Gong, *J. Mater. Chem. C*, 2015, **3**, 1794–1798.

69 Z.-L. Zhu, M. Chen, W.-C. Chen, S.-F. Ni, Y.-Y. Peng, C. Zhang, Q.-X. Tong, F. Lu and C.-S. Lee, *Org. Electron.*, 2016, **38**, 323–329.

View Article Online
DOI: 10.1039/C6SC05619A

Graphical Abstracts

Naphthyl-linked donor-π-acceptor fluorophores were utilized to achieve high performances and good color purity violet-blue emission in organic light-emitting devices (OLEDs).

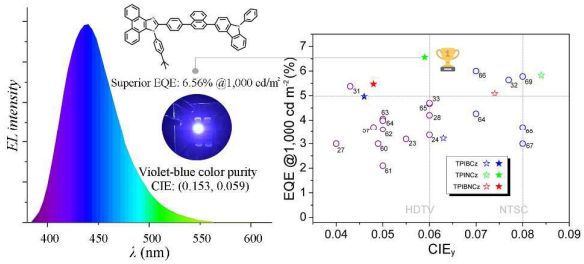

8.11 × 3.79 cm